

The study of the relationship between pore structure and photocatalysis of mesoporous TiO₂

BING GUO^a, HANGYAN SHEN^{a,*}, KANGYING SHU^a, YAOWU ZENG^b and WENSHENG NING^c

^aCollege of Materials Science and Engineering, China Jiliang University, Hangzhou 310018, China

^bCenter of Test and Analysis, Zhejiang University, Xixi Campus, Hangzhou 310028, China

^cCollege of Chemical Engineering and Materials, Zhejiang University of Technology, Hangzhou 310032, China

e-mail: shenhangyan@yahoo.com.cn

MS received 30 July 2008; revised 24 September 2008

Abstract. Mesoporous titania was synthesized by a sol–gel method using the surfactants Span85 and X114 as the template. The pore structure was determined by the N₂ adsorption/desorption method below 73 K and calculated using the BJH model. TEM characterizations show that the pores are formed through particle accumulation. Two kinds of channels, straight channels made of cylindrical capillaries and curved channels made of slit-shaped pores, exist in the bulk materials. The influence of the pore structure of mesoporous TiO₂ on its photocatalytic performance was studied. The sample with higher porosity, better textural properties and straight channels are good for photocatalytic performance.

Keywords. Mesoporous TiO₂; pore structure; photocatalytic performance.

1. Introduction

TiO₂ is an effective catalytic material and has been intensively studied for sensors,^{1,2} as a photocatalyst,³ in solar cells,⁴ lithium-ion cells⁵ and many others. Many studies have reported that the surface properties of TiO₂, including grain size, crystallization, morphology, specific surface area, surface state, and porosity clearly influence its photocatalytic activity.^{6–8}

Mesoporous TiO₂ has better properties in many respects than ordinary TiO₂ because of its high specific surface area and uniform pore diameter. Mesoporous TiO₂ was first synthesized through modified sol–gel routes in the presence of alkylphosphate surfactant templates in 1995.⁹ Since then, researchers have adopted different routes to the synthesis of TiO₂ with the mesoporous structure such as the hydrothermal process using cetyltrimethylammonium bromide (CTAB) as a template agent,¹⁰ the ultrasonic irradiation method,¹¹ the use of block copolymers,¹² the hydrolysis of TiOCl₂ aqueous solution at low temperature using octyl polyethylene oxide as the template agent,¹³ and so on. Though this

mesoporous TiO₂ has proved to have excellent performance as a photocatalyst there has been little investigation of the relationship between the pore structure and photocatalysis. In this paper, mesoporous TiO₂ was synthesized by the sol–gel method using tetrabutyl titanate as the precursor and Span85 or X114 as the surfactant. The pore structure of mesoporous TiO₂ was characterized by N₂ adsorption/desorption isotherms, X-ray diffraction (XRD), scanning electron microscopy (SEM) and transmission electron microscopy (TEM) methods. The influence of the pore structure of mesoporous TiO₂ on its photocatalytic performance was studied. The results show that the catalytic activity has a close relationship with the pore structure.

2. Experimental

2.1 Synthesis of mesoporous TiO₂

Mesoporous TiO₂ was synthesized by the sol–gel method. Span85(C₆₀H₁₀₈O₈) and X114(*t*-Oct-C₆H₄-(OCH₂CH₂)_xOH, *x* = 7–8) were chosen as the surfactants respectively. A homogeneous solution was obtained by stirring a mixture of 50 ml ethanol and surfactant. The dosage of Span85 and X114 are

*For correspondence

0.006 mol and 0.025 mol. 17 g tetrabutyl titanate was dropped into the above solution and then allowed to react at 60°C overnight. The resulting sol solution was gelled at 80°C in air for 7 days. Mesoporous TiO₂ was obtained by calcination of the gel at 500°C for 6 h in air to remove the surfactant species. The samples were designated as TiO₂-X114 and TiO₂-Span85 in this paper depending on the surfactant. TiO₂ is the nano-titania as purchased from Sinopharm Chemical Reagent Co., Ltd.

2.2 Photocatalytic performance

Photocatalytic performance was tested by a study of the photo-degradation of acetone. The content of produced CO₂ was analysed by a gas chromatograph GC112 equipped with a thermal conductivity detector (TCD) using TDX-101 as the chromatogram column.

2.3 Characterization

The N₂ adsorption/desorption isotherms of mesoporous titania were measured on a Micromeritics ASAP 2020 instrument at a temperature below 73 K. The sample was treated at 300°C before measurement. Surface areas of the samples were calculated from the adsorption isotherms by the BET method and the pore size distributions determined from desorption isotherms by the Barrett–Joiner–Halenda (BJH) method. The average pore size was calculated from the *t*-plot method.

XRD patterns of the samples were obtained on a Thermo ARL SCINTAG X'TRA X diffractometer (using CuK α radiation, $\lambda = 0.15406$ nm, scan range $2\theta = 15^\circ \sim 80^\circ$, scan rate = 0.02 s⁻¹).

TEM was conducted on a JEM2010 (HR) instrument. SEM was conducted on a Hitachi S-4700 instrument.

3. Results and discussion

3.1 Structure characterization

The XRD patterns of TiO₂-X114 and TiO₂-Span85 are shown in figure 1. The diffraction peaks at 25.28°, 37.80° and 48.05° are consistent with the (101), (004) and (200) peaks of anatase TiO₂. The XRD results suggest that the samples prepared in this work have good anatase crystallization and the kind

of surfactant has little influence on the nature of crystal formation.

Figure 2 shows the N₂ adsorption/desorption isotherms of TiO₂-X114, TiO₂-Span85 and TiO₂. The isotherms of TiO₂-X114 and TiO₂-Span85 are of type I¹⁴ and that of TiO₂ is of type II. During the process of adsorption, single molecular layer adsorption occurred at relatively low pressure and then multi-molecular layer adsorption occurred at higher pressure. The larger are the sample pore sizes, the higher the pressure of capillary cohesion that occurred.¹⁴ As shown in figure 2, the capillary cohesion of TiO₂ occurred at the highest pressure and that of TiO₂-Span85 occurred at the lowest pressure. It suggests that the sample TiO₂ had the largest pore size and TiO₂-Span85 had the smallest pore size. The hysteresis loop of TiO₂-X114 is the H1 type,¹⁴ which can originate from independent cylindrical capillaries. The hysteresis of nanometer TiO₂ is H3,¹⁴ which suggested that the sample has slit-

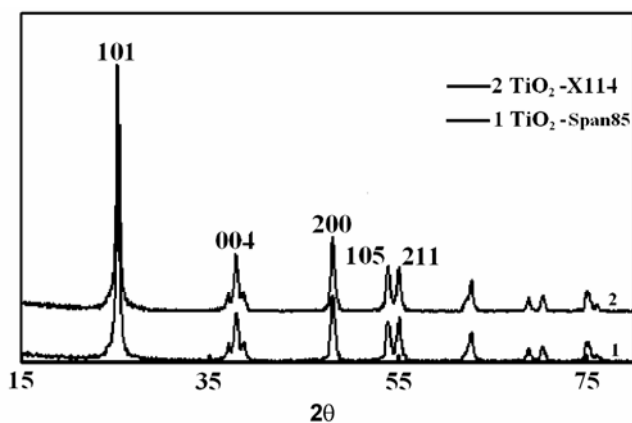


Figure 1. X-ray patterns of sample TiO₂-X114 and TiO₂-Span85.

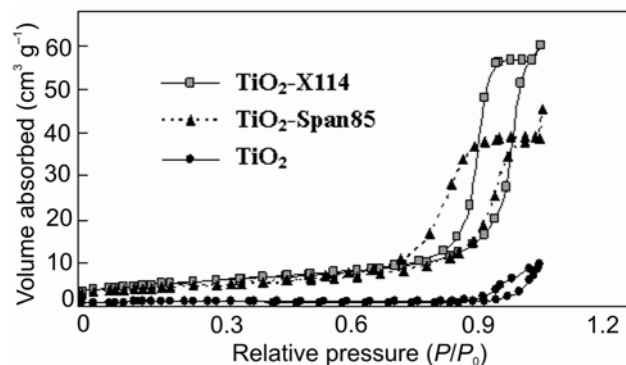


Figure 2. N₂ adsorption/desorption isotherms of TiO₂-X114, TiO₂-Span85 and TiO₂.

shaped pores. The hysteresis loop of TiO₂-Span85 is the H1 + H3 type, which indicated that this sample has some slit-shaped pores. Figure 3 is the pore size distribution of sample derived from the desorption

branch of the N₂ adsorption/desorption isotherm. Samples TiO₂-Span85 and TiO₂-X114 have a narrow pore size distribution and most of the pore diameters are in the range of 10–20 nm. The sample TiO₂ has a wide pore size distribution with most of the pore diameters in the range of 10–30 nm. The surface area, pore volume and the average pore size of samples

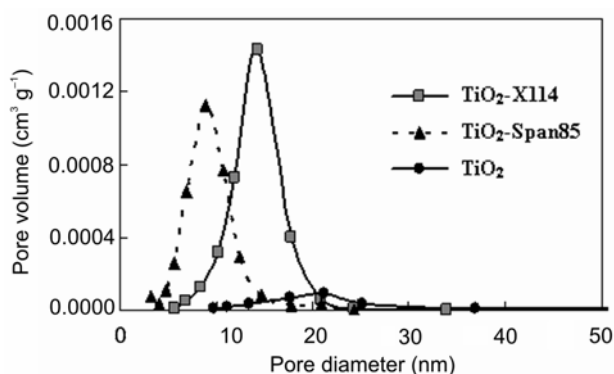
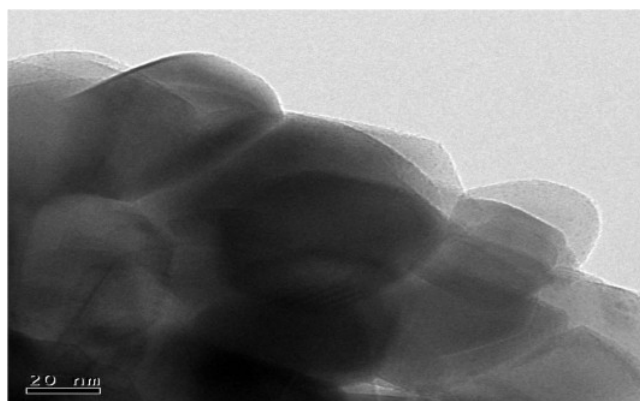
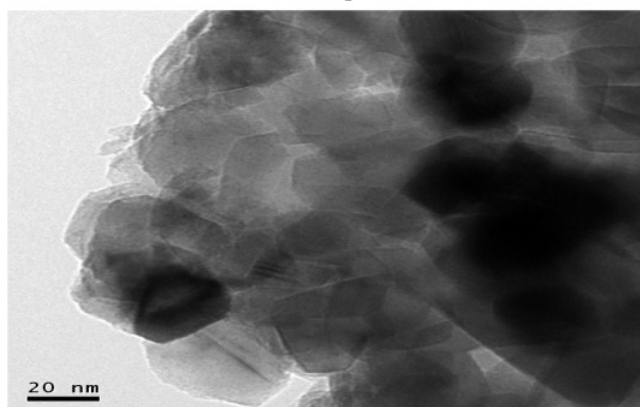


Figure 3. Pore size distributions of TiO₂-X114, TiO₂-Span85 and TiO₂ derived from desorption branches of N₂ adsorption/desorption isotherms.



TiO₂



TiO₂-Span85

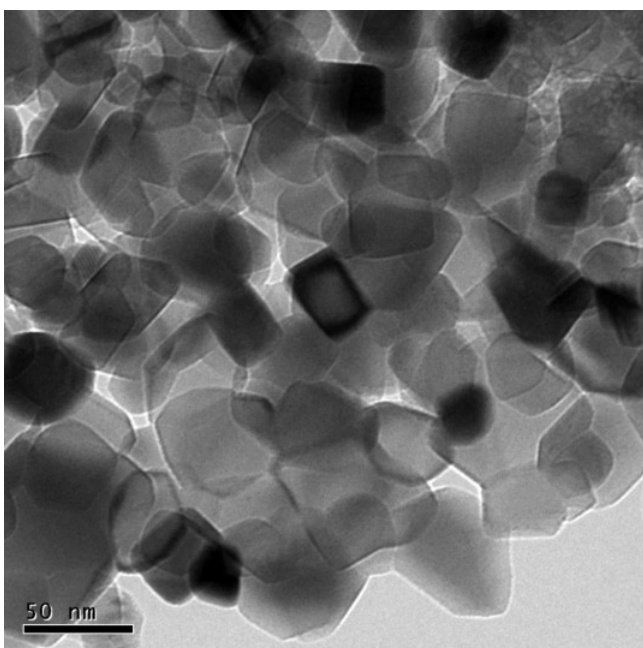
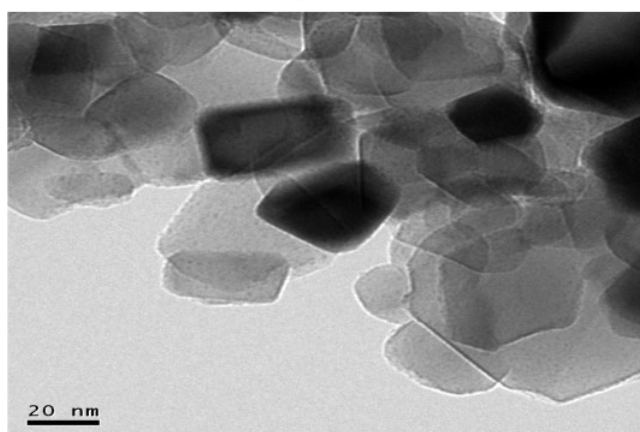


Figure 4. TEM image of sample TiO₂-X114.



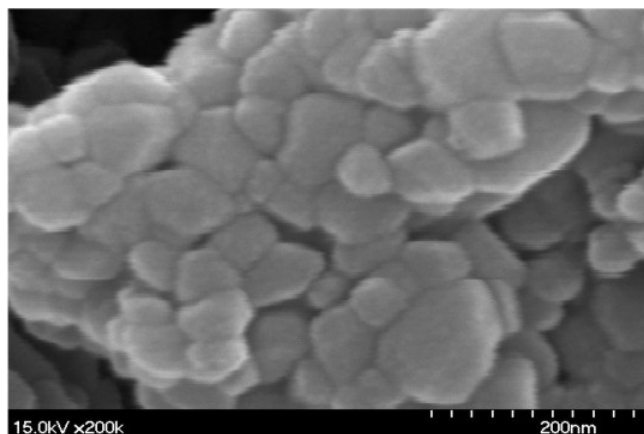
TiO₂-X114

Table 1. The specific surface area, pore volume and the average pore size of samples.

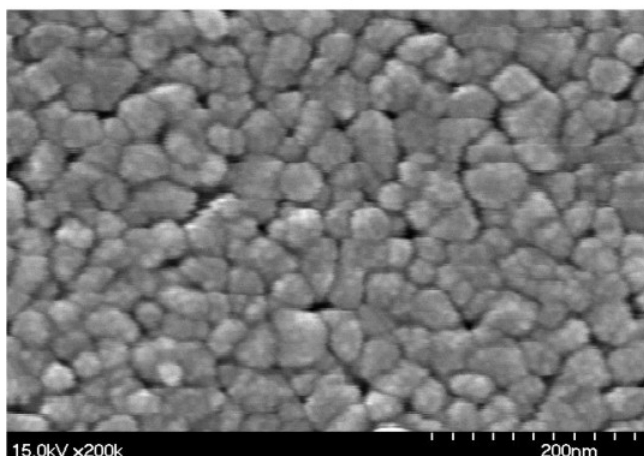
Sample	Surface area (m ² /g)	Pore volume (cm ³ /g)	Average pore size (nm)
TiO ₂ -X114	18.96	0.093	14.4
TiO ₂ -Span85	15.8	0.06	10.1
TiO ₂	3.58	0.0094	24.38

Figure 5. TEM images of TiO₂-X114, TiO₂-Span85 and TiO₂.

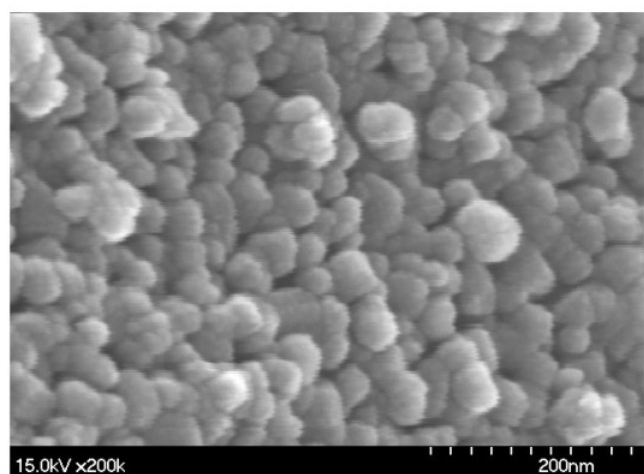
are summarized in table 1. Although the sample TiO_2 has the largest average pore size, its surface area and pore volume is smallest which indicated that the porosity is very low. The textural properties



TiO_2



TiO_2 -Span85



TiO_2 -X114

Figure 6. SEM images of TiO_2 -X114, TiO_2 -Span85 and TiO_2 .

of TiO_2 -X114 are greater than those of TiO_2 -Span85.

Figure 4 shows the TEM image of TiO_2 -X114. Nano-particles were packed randomly and pore channels were formed from the particle packing. The translucent region represents the straight channels and the gray region represents the curved channels. Figure 5 shows the TEM images of TiO_2 -X114, TiO_2 -Span85 and TiO_2 . It is clear that TiO_2 has many shadow regions indicating that the nano-particles have agglomerated. TiO_2 -X114 has much more translucent region than TiO_2 -Span85 which suggests that TiO_2 -X114 has many straight channels. TiO_2 -Span85 has much more gray regions which suggest that many curved channels were formed. The results of the TEM accord well with that of the N_2 adsorption/desorption test. The H3 hysteresis loop of TiO_2 suggested that there are curved channels in the bulk. TiO_2 -Span85 has many curved channels consisting mainly of slit-shaped pores. TiO_2 -X114 has many straight channels consisting mainly of independent cylindrical capillaries.

Figure 6 shows the SEM images of TiO_2 -X114, TiO_2 -Span85 and TiO_2 . It indicates that particles of TiO_2 congregate together so densely that few gaps exist between the pores. In contrast, the particles of TiO_2 -X114 and TiO_2 -Span85 congregate loosely. The particle size of TiO_2 -X114 is slightly larger than that of TiO_2 -Span85. The agglomeration of TiO_2 particles resulted in have low surface area and pore volume.

3.3 Photocatalytic activity

The pore-structure of mesoporous TiO_2 influences the adsorption of photoelectrons, reagents and prod-

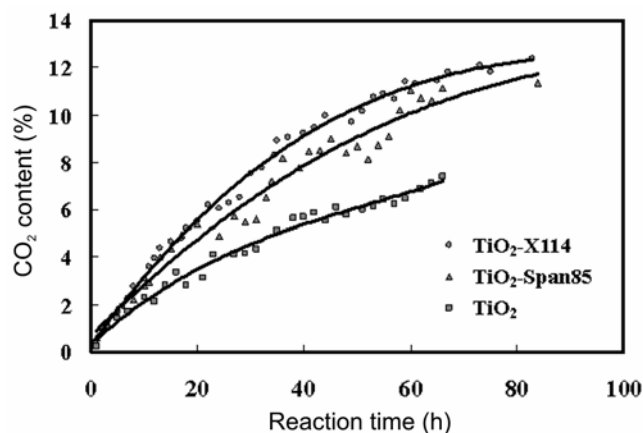


Figure 7. Photocatalytic performances of TiO_2 -X114, TiO_2 -Span85 and TiO_2 .

ucts on the surface site. As a result, the photocatalytic activity of mesoporous TiO₂ will change with its pore structure. Figure 7 shows the dependence of the content of product CO₂ on the reaction time. The photocatalytic activity of nanometer TiO₂ is lower than that of mesoporous TiO₂-X114 and TiO₂-Span85. From the structure data, nanometer TiO₂ has many slit-gap pores with a H3 hysteresis loop and low porosity resulting in its small surface area and pore volume. Its structure is not suitable for the adsorption of photoelectrons and the diffusion of reagent and product. TiO₂-Span85 has many curved channels, a lower specific surface area, smaller pore volume and narrower pore diameter than TiO₂-X114, which limit the diffusion of reagent and product. As a result, TiO₂-Span85 has lower photocatalytic performance than that of TiO₂-X114.

4. Conclusions

In this paper, mesoporous TiO₂ was synthesized using the sol-gel method with surfactants Span85 and X114. The pore structures of the samples were determined by N₂ adsorption/desorption isotherms and TEM methods. Results indicated that the particles of mesoporous TiO₂ are arranged randomly and the pore channels are formed from the packing of particles. Two kinds of pore channels exist in the bulk samples. One is the curved channel composed mainly of slit-shaped pores. Another is the straight channel mainly formed by independent cylindrical capillaries. The photocatalytic activity of mesoporous TiO₂ has a close relationship to its pore structure. The sample with higher porosity, better textural properties and straight channel are good for photocatalytic performance. More detailed research into the dependence of pore structure on the photocatalytic activity is under investigation.

Acknowledgements

This work was financially supported by the National Science Foundation of China (no. 20701034) and Zhejiang Provincial Top Discipline.

References

1. Savage N, Chwieroth B, Ginwalla A, Patton B R, Akbar S A and Dutta P K 2001 *Sens. Actuator* **B79** 17
2. Yasuhiro Shimizu, Takeo Hyodo and Makoto Egashira 2004 *Eur. Ceram. Soc.* **24** 1389
3. Yu J C, Yu J, Ho W and Zhao J 2002 *J. Photochem. Photobiol., A Chem.* **148** 331
4. George Phani, Gavin Tulloch, David Vittorio and Igor Skryabin 2001 *Renew Energy* **22** 303
5. Kavan L, Rathouský J, Grätzel M, Shklover V and Zukal A 2001 *Microporous Mesoporous Mater.* **44-45** 653
6. Subramanian V, Wolf E E and Kamat P V 2004 *J. Am. Chem. Soc.* **126** 4943
7. Ohtani B, Ogawa Y and Nishimoto S 1997 *J. Phys. Chem.* **B101** 3746
8. Yu J G, Wang B, Cheng M and Zhou 2007 *Appl. Catal. B: Environ.* **69** 171
9. Antonelli D M and Ying J Y 1995 *Angew. Chem. Int. Ed.* **34** 2014
10. Peng T Y, Zhao D, Dai K, Shi W and Hirao K 2005 *Phys. Chem.* **B109** 4947
11. Yu J, Yu J C, Lueng M K P, Ho W, Cheng B, Zhao X and Zhao J 2003 *J. Catal.* **217** 69
12. Smarsly B, Grosso D, Brezesinski T, Pinna N, Boissiere C, Antonietti M and Sanchez C 2004 *Chem. Mater.* **16** 2948
13. Li Y, Lee N H, Lee E G, Song J S and Kim S J 2004 *Chem. Phys. Lett.* **389** 124
14. Rojas F, Kornhauser I, Felipe C, Esparza J M, Cordero S, Dominguez A and Riccardo J L 002 *Phys. Chem. Chem. Phys.* **4** 2346